^{33}S hyperfine interactions in H_2S and SO_2 and revision of the sulfur nuclear magnetic shielding scale

Trygve Helgaker,[1,a)] Jürgen Gauss,[2,b)] Gabriele Cazzoli,[3,c)] and Cristina Puzzarini[3,d)]
[1]*Centre for Theoretical and Computational Chemistry, Department of Chemistry, University of Oslo, N-0315 Oslo, Norway*
[2]*Institut für Physikalische Chemie, Universität Mainz, D-55099 Mainz, Germany*
[3]*Dipartimento di Chimica "Giacomo Ciamician," Università di Bologna, Via Selmi 2, I-40126 Bologna, Italy*

(Received 25 September 2013; accepted 3 December 2013; published online 30 December 2013)

Using the Lamb-dip technique, the hyperfine structure in the rotational spectra of $H_2{}^{33}S$ and $^{33}SO_2$ has been resolved and the corresponding parameters—that is, the sulfur quadrupole-coupling and spin–rotation tensors—were determined. The experimental parameters are in good agreement with results from high-level coupled-cluster calculations, provided that up to quadruple excitations are considered in the cluster operator, sufficiently large basis sets are used, and vibrational corrections are accounted for. The ^{33}S spin-rotation tensor for H_2S has been used to establish a new sulfur nuclear magnetic shielding scale, combining the paramagnetic part of the shielding as obtained from the spin–rotation tensor with a calculated value for the diamagnetic part as well as computed vibrational and temperature corrections. The value of 716(5) ppm obtained in this way for the sulfur shielding of H_2S is in good agreement with results from high-accuracy quantum-chemical calculations but leads to a shielding scale that is about 28 ppm lower than the one suggested previously in the literature, based on the ^{33}S spin-rotation constant of OCS. © *2013 AIP Publishing LLC*. [http://dx.doi.org/10.1063/1.4849177]

INTRODUCTION

The determination of nuclear shielding constants by means of nuclear-magnetic-resonance (NMR) spectroscopy requires the use of an accurate reference standard for each nuclide to which the measured chemical shifts can be related. The shieldings of these references are obtained from investigations of nuclear spin–rotation interactions in rotational spectra.[1,2] Their analysis provides the paramagnetic part of the shielding, which is subsequently combined with a theoretical value for the diamagnetic contribution.

In a recent benchmark study of calculated NMR shielding and spin–rotation constants for 28 mostly small organic molecules,[3] it became clear that the agreement between measured and calculated shielding constants is poorer for ^{33}S than for other nuclei in the study. Specifically, at the extrapolated all-electron CCSD(T) level of theory (CCSD(T)/aug-cc-pCV[TQ]Z), the calculated equilibrium shielding constants of ^{33}S are 739.1, 796.7, and −203.5 ppm for H_2S, OCS, and SO_2, respectively, while the corresponding experimental values (corrected for vibrations using B3LYP/aug-cc-pCVTZ calculations) are 733.9, 834.3, and −139.6 ppm. These experimental values are relative to the shielding scale by Jackowski *et al.*,[4,5] based on an absolute shielding of 817(12) ppm in OCS, obtained from a measured spin–rotation constant by Reinartz and Dymanus[6] and a quantum-chemically calculated diamagnetic contribution, but without a proper treatment of ro-vibrational effects. Based on the same OCS measurements, an absolute ^{33}S shielding of 843(12) ppm had been proposed earlier by Wasylishen, Connor, and Friedrich.[7] The corresponding computed vibrationally averaged shielding of OCS obtained in Ref. 3 is 779.4 ppm. The large difference of 38 ppm between calculated and measured shieldings of ^{33}S in the reference compound OCS (about 5%) indicates that further investigations are needed to establish an accurate shielding scale for this nucleus. Although such a shielding scale is not essential for standard NMR measurements, it has relevance for the computation of NMR shieldings.[1] There, the knowledge of experimental absolute shieldings is necessary to quantify the remaining errors in the quantum-chemical treatments; those errors are often not apparent when comparing relative shifts.

In an attempt to establish a more accurate ^{33}S shielding scale, we present in this paper new experimental measurements of the spin–rotation constants of $H_2{}^{33}S$ and $^{33}SO_2$. These nonlinear molecules are potentially better suited for establishing an accurate shielding scale of ^{33}S than OCS, for which a reliable calculation of the vibrational correction to the spin–rotation constants is currently not feasible because of linearity—without an estimate of this correction, an accurate absolute shielding constant cannot be derived. In conjunction with the new measurements on $H_2{}^{33}S$ and $^{33}SO_2$, we present high-level quantum-chemical calculations for these systems—in particular, for their equilibrium and vibrationally averaged ^{33}S spin–rotation and shielding constants. By combining the measured spin–rotation constant for H_2S with the results of high-level *ab initio* calculations, we arrive at an absolute isotropic shielding constant of 716(5) ppm for ^{33}S in H_2S.

a)Electronic mail: t.u.helgaker@kjemi.uio.no
b)Electronic mail: gauss@uni-mainz.de
c)Electronic mail: gabriele.cazzoli@unibo.it
d)Electronic mail: cristina.puzzarini@unibo.it

EXPERIMENTAL MEASUREMENTS

Measurements were performed with a frequency-modulated computer-controlled spectrometer working from 65 GHz to 1.6 THz,[8,9] with the 200–450 GHz frequency range actually considered. The Lamb-dip technique[10,11] (in conjunction with a conventional free-space cell[12] with a double-path arrangement[13]) was exploited to obtain sub-Doppler resolution, and thus to resolve the hyperfine structure due to ^{33}S. Concerning the experimental details, the millimeter- and submillimeter-wave sources employed, phase-locked to a rubidium frequency standard, were frequency multipliers driven by Gunn diode oscillators. The frequency modulation was obtained by sine-wave modulating at 1.66 kHz the 72 MHz local oscillator of the synchronization loop (with the modulation depth varied from 36 to 60 kHz, according to the transition under consideration). Schottky diode detectors were used, and their output processed by means of a Lock-in amplifier tuned to twice the modulation frequency, thus recording the second derivative of the natural line profile. With respect to the experimental conditions, being interested in the ^{33}S-containing isotopologues, measurements were performed in natural abundance (0.76%), using commercial samples, both in static conditions and in a continuous flow of gas, maintained by a diffusion pump. Low-pressure values (0.5–1 mTorr) were chosen to minimize the dip widths as much as possible to improve the resolution as well as to avoid frequency shifts. On the whole, a total of 65 and 45 distinct frequency lines could be assigned to $H_2{}^{33}S$ and $^{33}SO_2$, respectively, with the frequency values obtained by means of line-profile analysis[14,15] and as averages of several sets of measurements. On the basis of the standard deviations of these averages, the transition intensities, and the signal-to-noise ratio,[16,17] a conservative estimate of the experimental uncertainty is 2 kHz.

Figure 1, which depicts the hyperfine structure of the $J = 3_{2,1} \leftarrow 3_{1,2}$ rotational transition of $H_2{}^{33}S$, and Figure 2, which shows the hyperfine structure of the $J = 17_{1,17} \leftarrow 16_{0,16}$ transition of $^{33}SO_2$, demonstrate the high resolution provided by the Lamb-dip technique even in the case of ^{33}S-containing compounds investigated in natural abundance. In addition, the inset of Figure 2 demonstrates the importance of properly choosing experimental parameters such as the modulation depth to resolve the hyperfine structure best.

The transition-frequency values of $H_2{}^{33}S$ and $^{33}SO_2$ were included in nonlinear least-squares fits, in which they were weighted proportionally to the inverse square of their experimental uncertainty. For unresolved hyperfine components, the calculated frequencies were evaluated using intensity-weighted averages. In the fitting procedures, the rotational and quartic centrifugal-distortion constants together with the hyperfine parameters were determined, while the high-order centrifugal-distortion constants were kept fixed. For $^{33}SO_2$, the corresponding values were taken from Ref. 18, while for $H_2{}^{33}S$ the values determined in a global fit (including old

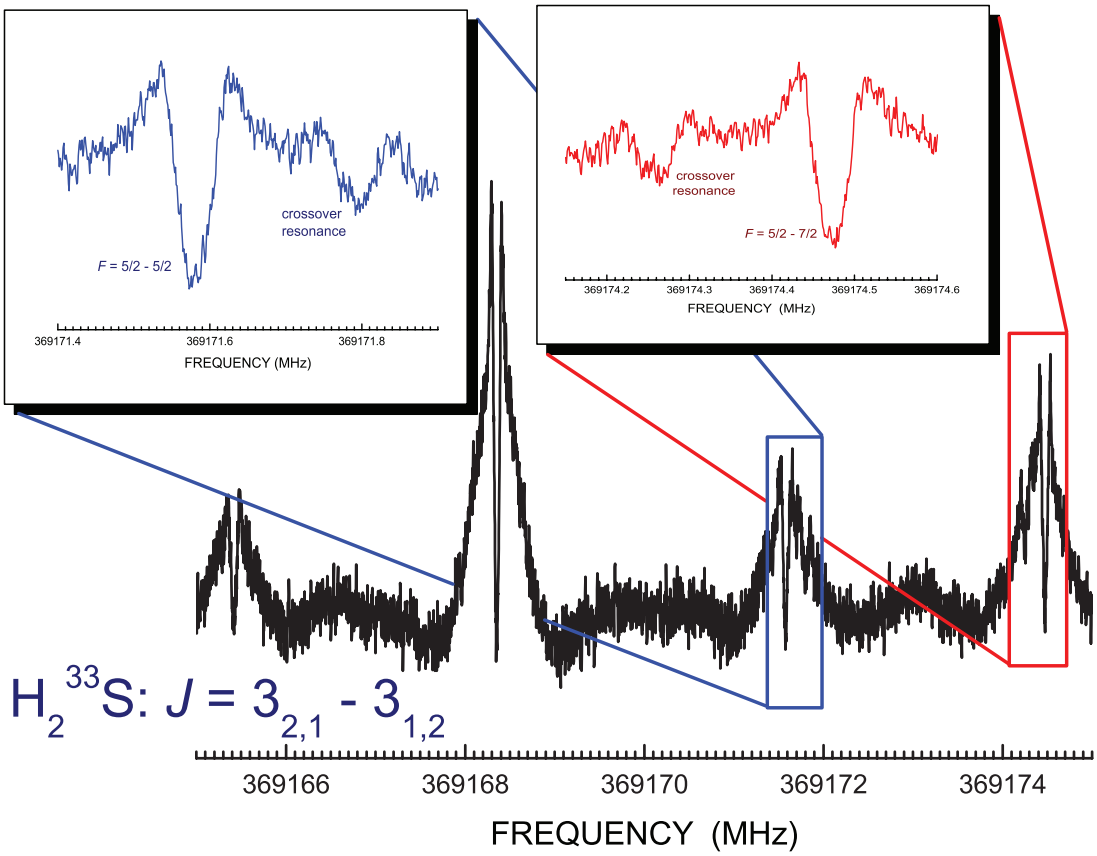

FIG. 1. The hyperfine structure of the $J = 3_{2,1} \leftarrow 3_{1,2}$ rotational transition of $H_2{}^{33}S$ (P = 1 mTorr, mod. depth = 60 kHz). In the insets, the $F = 5/2 - 5/2$ (P = 1 mTorr, mod. depth = 45 kHz) and $F = 5/2 - 7/2$ (P = 1 mTorr, mod. depth = 36 kHz) hyperfine components are shown in details together with crossover resonances (experimental artefacts due to the saturation of overlapping Gaussian profiles).

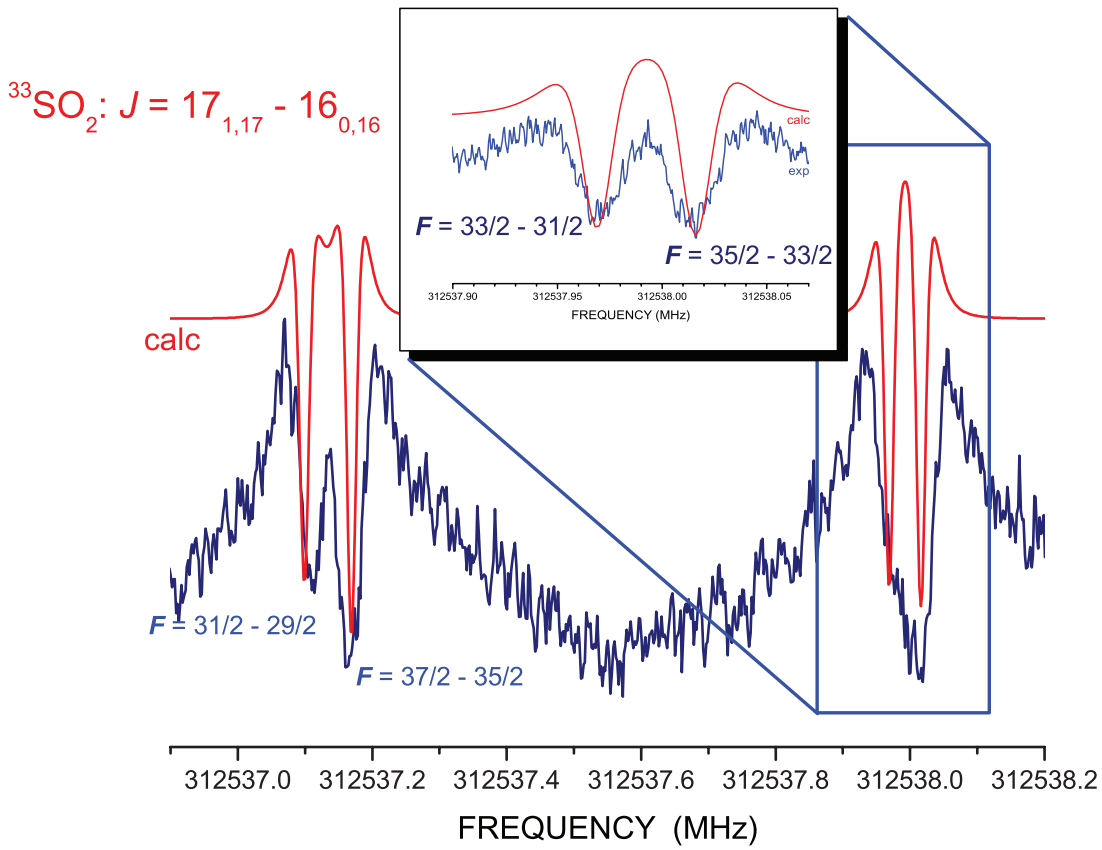

FIG. 2. The hyperfine structure of the $J = 17_{1,17} \leftarrow 16_{0,16}$ rotational transition of $^{33}SO_2$ (P = 1 mTorr, mod. depth = 36 kHz): the dips at the center of the Gaussian profiles are evident. In the inset, the $F = 33/2 - 31/2$ and $F = 35/2 - 33/2$ hyperfine components are resolved by reducing the modulation depth (P = 1 mTorr, mod. depth = 24 kHz). The simulation based on the computed hyperfine parameters is depicted in red.

and new, improved measurements[19]) were used. The fits were performed with Pickett's SPFIT program,[20,21] employing Watson's *A*-reduced Hamiltonian in the I^r representation.[22] We finally note that for $^{33}SO_2$ we also included the hyperfine components of the $J = 1_{1,1} \leftarrow 2_{0,2}$ transition from Ref. 18 in the fitting procedure, being the only previous sub-Doppler measurements available in the literature.

QUANTUM-CHEMICAL CALCULATIONS

The NMR shielding tensor $\boldsymbol{\sigma}_K$ and spin–rotation tensor $\mathbf{C}_K$ are second-order magnetic properties and may be identified as the following derivatives of the molecular electronic energy:[23,24]

$$\boldsymbol{\sigma}_K = \left.\frac{\mathrm{d}^2 E}{\mathrm{d}\mathbf{B}\mathrm{d}\mathbf{m}_K}\right|_{\mathbf{B},\mathbf{m}_K=\mathbf{0}}, \tag{1}$$

$$\mathbf{C}_K = \left.\frac{\mathrm{d}^2 E}{\mathrm{d}\mathbf{J}\mathrm{d}\mathbf{I}_K}\right|_{\mathbf{J},\mathbf{I}_K=\mathbf{0}}, \tag{2}$$

where E is the electronic energy (excluding the nuclear spin–Zeeman term), $\mathbf{B}$ is the external magnetic field, $\mathbf{J}$ is the rotational angular momentum, and $\mathbf{m}_K = \gamma_K \mathbf{I}_K$ is the magnetic moment associated with nucleus K of nuclear spin $\mathbf{I}_K$ and gyromagnetic ratio γ_K. In these equations and throughout this paper, atomic units are used unless otherwise stated. It is important to note that different sign conventions exist for the spin–rotation constant. We here follow the convention adopted in most recent experimental papers, which differs from the one used by Flygare in his classic papers.[25,26]

In all of our calculations, we use London atomic orbitals (LAOs),[27] also known as gauge-including atomic orbitals (GIAOs). The use of these orbitals for calculating magnetic properties involving an external magnetic field is now standard and preferable to other procedures for imposing gauge-origin independence because of its rapid basis-set convergence.[23,24,28] For rotating molecules, the rotational LAOs are defined as[29]

$$\omega_\mu(\mathbf{B},\mathbf{J},\mathbf{r}) = \mathrm{e}^{-\mathrm{i}\left(\frac{1}{2}\mathbf{B}\times(\mathbf{R}_\mu-\mathbf{R}_\mathrm{O})-\mathbf{I}^{-1}\mathbf{J}\times\mathbf{R}_\mu\right)\cdot\mathbf{r}}\chi_\mu(\mathbf{r}), \tag{3}$$

where $\chi_\mu(\mathbf{r})$ denotes the usual atomic basis functions centered at $\mathbf{R}_\mu$, $\mathbf{R}_\mathrm{O}$ is the origin of the vector potential, and $\mathbf{I}^{-1}$ is the inverse moment-of-inertia tensor. When LAOs are used, the relation between the paramagnetic contribution to the shielding tensor and the spin–rotation tensor is[29]

$$\mathbf{C}_K = 2\gamma_K\left(\boldsymbol{\sigma}_K^{\mathrm{LAO}} - \boldsymbol{\sigma}_K^{\mathrm{d}}(\mathbf{R}_K)\right)\mathbf{I}^{-1} + \mathbf{C}_K^{\mathrm{n}}, \tag{4}$$

where $\boldsymbol{\sigma}_K^{\mathrm{LAO}}$ is the shielding tensor calculated using LAOs, $\boldsymbol{\sigma}_K^{\mathrm{d}}(\mathbf{R}_K)$ is the diamagnetic contribution to the shielding tensor calculated with standard atomic orbitals and the gauge origin at $\mathbf{R}_K$ (the position of nucleus K), and $\mathbf{C}_K^{\mathrm{n}}$ is the nuclear contribution to the spin–rotation tensor.

The quantum-chemical results presented in the following have been obtained using the restricted Hartree–Fock (RHF), coupled-cluster singles-doubles (CCSD),[30] coupled-cluster

singles-doubles-triples (CCSDT),[31,32] and coupled-cluster singles-doubles-triples-quadruples (CCSDTQ) models.[33] In addition, we employ second-order Møller–Plesset (MP2) theory[34] as an approximation to the CCSD model, while the CCSD method augmented by a perturbative treatment of triple excitations (CCSD(T)) serves as an approximation to the CCSDT method.[35] The CFOUR program package[36] was used for all calculations in the present study except those carried out at the CCSDTQ level, which were performed with the MRCC program[37] interfaced to CFOUR.

Computational protocol for geometrical properties

For the geometrical properties (equilibrium geometries and rotational constants), we used the following composite energy:[38]

$$E_{\text{tot}} = E^{\infty}_{\text{RHF}} + \Delta E^{\infty}_{\text{fc-CCSD(T)}} + \Delta E^{\text{TZ}}_{\text{T}} + \Delta E^{\text{DZ}}_{\text{Q}} + \Delta E^{\text{5Z}}_{\text{core}}, \tag{5}$$

where E^{∞}_{RHF} is the basis-set-limit Hartree–Fock energy calculated using Feller's exponential formula[39] with the correlation-consistent cc-pVQZ, cc-pV5Z, and cc-pV6Z basis sets,[40–43] while $\Delta E^{\infty}_{\text{fc-CCSD(T)}}$ is the frozen-core (fc) CCSD(T) correlation energy extrapolated to the complete basis-set (CBS) limit using the two-point X^{-3} extrapolation formula[44] with the cc-pV5Z and cc-pV6Z basis sets. The remaining higher-order corrections for full triples, quadruples, and core-correlation are given by

$$\Delta E^{\text{TZ}}_{\text{T}} = E^{\text{cc-pVTZ}}_{\text{fc-CCSDT}} - E^{\text{cc-pVTZ}}_{\text{fc-CCSD(T)}}, \tag{6}$$

$$\Delta E^{\text{DZ}}_{\text{Q}} = E^{\text{cc-pVDZ}}_{\text{fc-CCSDTQ}} - E^{\text{cc-pVDZ}}_{\text{fc-CCSDT}}, \tag{7}$$

$$\Delta E^{\text{5Z}}_{\text{core}} = E^{\text{cc-pCV5Z}}_{\text{ae-CCSD(T)}} - E^{\text{cc-pCV5Z}}_{\text{fc-CCSD(T)}}. \tag{8}$$

The resulting equilibrium geometries determined using analytical gradients based on Eq. (5) are highly accurate, yielding bond distances within 0.1 ppm of the exact result.[38]

The equilibrium structures obtained as described above were used to calculate equilibrium values of the rotational constants, subsequently corrected for molecular vibrations. The vibrational corrections were computed by second–order vibrational perturbation theory (VPT2)[45,46] at the frozen-core CCSD(T)/cc-pV*X*Z levels with $X = 3, 4$. In addition, quartic centrifugal-distortion constants were obtained using standard formulas from the available harmonic force fields, while quadrupole-coupling constants were obtained from electric-field gradients calculated at the all-electron (ae) CCSD(T)/cc-pCV*X*Z levels with $X = 4, 5$, using a value for the ^{33}S nuclear quadrupole moment of -69.4 mb.[47] The reported values for the quadrupole-coupling constants were vibrationally corrected using VPT2 as described in Ref. 46.

Computational protocol for magnetic properties

For the spin–rotation and shielding tensors, we carried out all-electron MP2, CCSD, CCSD(T), CCSDT, and CCSDTQ calculations[48–52] in the correlation-consistent core–valence basis sets cc-pCV*X*Z[53,54] and in the corresponding augmented (with diffuse functions) basis sets aug-cc-pCV*X*Z,[42,55] with cardinal numbers $3 \le X \le 5$. Whereas core orbitals are essential for an accurate calculation of these constants, the diffuse functions included in the aug-cc-pCV*X*Z basis sets are less important.

As discussed later, the CCSD(T)/cc-pCV*X*Z and CCSD(T)/aug-cc-pCV*X*Z calculations carried out at the equilibrium geometries of the composite energy in Eq. (5) provide highly accurate spin–rotation and shielding constants. For even higher accuracy, additional CCSDT and CCSDTQ calculations were carried out. Because of their high cost, these calculations had to be limited to smaller basis sets. For H_2S, the CCSD(T)/aug-cc-pCV5Z results were augmented by corrections due to the full treatment of triple excitations at the CCSDT/aug-cc-pCVQZ level and by corrections due to quadruples at the frozen-core CCSDTQ/cc-pCVTZ level, while for SO_2 the CCSD(T)/aug-cc-pCV5Z results could only be improved upon by corrections obtained at the CCSDT/cc-pCVTZ and frozen-core CCSDTQ/cc-pCVDZ levels. We note that double-zeta basis sets are in general unsuitable for high-accuracy calculations but their use makes sense in a composite scheme for evaluating high-excitation contributions. Finally, vibrational VPT2 corrections were computed at the fc-CCSD(T)/cc-pV*X*Z and all-electron CCSD(T)/(aug)-cc-pCV*X*Z levels, with $X = 3, 4$.

Calculations of the ^{33}S shielding tensor were also carried out for OCS (the reference compound for the previous sulfur shielding scales[5,7]) in the same way as for H_2S and S_2O. The CCSDT calculations were carried for OCS using the cc-pCVDZ and cc-pCVTZ basis sets, while the CCSDTQ calculations were limited to cc-pCVDZ basis and the frozen-core approximation.

RESULTS AND DISCUSSION

^{33}S spin–rotation tensors

The spectroscopic and hyperfine parameters experimentally determined in this work are collected in Table I, where they are compared with previous experimental data[18,56] and the corresponding computed values. The theoretical best-estimate geometries determined by the composite scheme described above and used in the quantum-chemical calculations of spin–rotation and shielding constants are also listed.

Considering the experimental results in Table I first and focusing on the spin–rotation constants, we note that, with respect to the literature, we have improved only the accuracy for $^{33}SO_2$, reducing the uncertainties by a factor of two to four. The situation is very different for $H_2{}^{33}S$, as the values in Ref. 56 turned out to be not only poorly determined, but also unreliable, most likely due to the lack of sub-Doppler measurements.[56] The experimental spin–rotation constants were determined in the present work with uncertainties of a few tenths of a kHz, sufficiently accurate for the subsequent determination of magnetic shieldings and an absolute ^{33}S NMR scale.

TABLE I. Geometrical parameters, spectroscopic constants,[a] and ^{33}S hyperfine parameters of $H_2{}^{33}S$ and $^{33}SO_2$.

	$H_2{}^{33}S$			$^{33}SO_2$		
Parameters	This work (exp)	Ref. 56	This work (calc)	This work (exp)	Ref. 18	This work (calc)
r_e (Å)	…	…	1.3358[b]	…	…	1.4307[b]
$\angle_e$ (deg)	…	…	92.33[b]	…	…	119.27[b]
A_e (MHz)	…	…	310836.7[b]	…	…	59514.7[b]
B_e (MHz)	…	…	270022.6[b]	…	…	10367.7[b]
C_e (MHz)	…	…	144497.9[b]	…	…	8829.6 [b]
A_0 (MHz)	310032.4195(39)	310032.415(16)	310522.9[c]	59856.4829(20)	59856.4785(18)	59766.4[c]
B_0 (MHz)	270356.5720(28)	270356.593(23)	269774.8[c]	10318.29909(32)	10318.29808(36)	10328.0[c]
C_0 (MHz)	141707.8910(14)	141707.919(18)	141766.6[c]	8780.13925(21)	8780.13926(38)	8785.9[c]
D_J (MHz)	19.56765(37)	19.5716(10)	17.7822[d]	0.0065930(10)	0.00659026(61)	0.00645006[d]
D_{JK} (MHz)	− 68.3432(18)	− 68.3324(24)	− 61.1947[d]	− 0.114242(16)	− 0.1142166(55)	− 0.106532[d]
D_K (MHz)	110.7982(14)	110.7785(21)	99.9469[d]	2.51397(84)	2.512337(30)	2.20964[d]
d_J (MHz)	8.86080(25)	8.86103(58)	7.99661[d]	0.00171232(16)	0.00171161(19)	0.00168318[d]
d_K (MHz)	− 4.02320(83)	− 4.0256(16)	− 5.50501[d]	0.024959(15)	0.025003(24)	0.0214504[d]
χ_{aa} (MHz)	− 32.8023(80)	− 32.820(53)	− 32.88[e]	− 1.8471(15)	− 1.8464(14)	− 1.59[e]
χ_{bb} (MHz)	− 8.6620(85)	− 8.597(66)	− 8.51[e]	25.6994(13)	25.7002(12)	25.90[e]
χ_{cc} (MHz)	41.4643(85)	41.416(56)	41.39[e]	− 23.8523(13)	− 23.8538(22)	− 24.31[e]
C_{aa} (kHz)	22.08(27)	8.4(72)	21.42[f]	39.79(37)	39.56(71)	39.10[f]
C_{bb} (kHz)	59.05(26)	52.0(86)	58.75[f]	5.85(16)	5.60(66)	5.79[f]
C_{cc} (kHz)	24.30(77)	22.2(72)	24.15[f]	4.38(14)	4.63(64)	4.34[f]
$\overline{\chi^2}$ [g]	0.96	…	…	0.99	…	

[a]Only the determined parameters are reported.
[b]Theoretical best estimates obtained using the composite scheme described in the text.
[c]Obtained by adding vibrational corrections (VPT2 at the fc-CCSD(T)/cc-pVQZ level of theory) to the equilibrium values.
[d]Obtained from the fc-CCSD(T)/cc-pVQZ harmonic force field.
[e]CCSD(T)/cc-pCV5Z equilibrium values augmented by vibrational corrections (fc-CCSD(T)/cc-pVQZ for the force field and CCSD(T)/cc-pCVQZ level for the property).
[f]Equilibrium best-estimate value (see text) augmented by vibrational corrections obtained at the CCSD(T)/aug-cc-pCVQZ level ($H_2{}^{33}S$) and the fc-CCSD(T)/cc-pVQZ level (SO_2).
[g]Dimensionless (weighted) standard deviation.

Regarding the computed results in Table I, we find that these show a satisfactory agreement with the available experimental data. For the rotational constants, the discrepancies are of the order of 0.05% to 0.2%, whereas, as usual, the accuracy of the centrifugal-distortion constants is lower, with deviations of about 10%. A quantitative agreement is noted for the quadrupole-coupling and spin–rotation constants. For these two constants, the inclusion of vibrational corrections turns out to be essential to reach this level of agreement—in particular, for the sulfur spin–rotation constants, which are the focus of the present study, the discrepancies are smaller than 1 kHz and thus well within the experimental uncertainties.

Tables II and III contain the results of our extensive computational investigation of electron-correlation and basis-set effects on the ^{33}S spin–rotation constants of H_2S and SO_2, respectively. Concerning the quantum-chemical treatment, the general trend is that inclusion of electron correlation decreases the absolute values of the spin–rotation constants. From an inspection of the results in the series RHF, CCSD, and CCSDT, we note that the largest effect is, as expected, due to single and double excitations, with contributions up to 10%. The inclusion of triple excitations tends to further reduce the absolute value, with corrections on the order of 1%. From the few CCSDTQ results available, we note that this trend continues when quadruple excitations are included in the coupled-cluster treatment, but the effects are only on the order of 0.1% or less.

Regarding the perturbative treatment of electron correlation, we find that the MP2 method overestimates the effect of double excitations on the spin–rotation constants, by 4% to 10% relative to the CCSD method. The CCSD(T) method likewise overestimates the effect of triple excitations slightly, thereby fortuitously providing a better description of the spin–rotation interactions than does the full CCSDT method.

Turning to a comparison of the results obtained with the different basis sets, we note a monotonic convergence of the spin–rotation constants in the aug-cc-pCV*X*Z series, the absolute value increasing with increasing cardinal number *X*. In the cc-pCV*X*Z series, the same trend is observed except for some oscillations in C_{aa} and C_{bb} for H_2S. Nevertheless, for both basis-set hierarchies, the spin–rotation constants obtained with the quadruple- and quintuple-zeta sets differ by only about 0.3%. The values computed with cardinal number $X = 5$ therefore seem to be well converged and can be considered good estimates for the CBS values.

From a comparison of the results obtained within the two basis-set hierarchies, the effect of diffuse functions can be inferred as well. As expected, the two series converge to the same limit. At the quintuple-zeta level, the differences are entirely negligible for SO_2, while for H_2S discrepancies of 0.1–0.2 kHz are observed for C_{aa} and C_{bb}. For the smaller cc-pCVTZ and aug-cc-pCVTZ sets, the differences are small (a few hundredths of a kHz) for SO_2, while they can be as large as 1 kHz for H_2S. We also note that the

TABLE II. Computed ^{33}S spin–rotation constants (in kHz) for H_2S.[a]

	RHF	MP2	CCSD	CCSD(T)	CCSDT	CCSDTQ
C_{aa}						
cc-pCVDZ	18.969	17.066	18.544	18.745	18.835	18.815
cc-pCVTZ	19.219	17.537	19.196	19.218	19.327	
					(18.975)	(18.954)
cc-pCVQZ	19.057	17.236	18.906	18.886	18.999	
cc-pCV5Z	18.912	17.023	18.724	18.671		
aug-cc-pCVTZ	18.558	16.472	18.299	18.260	18.373	
aug-cc-pCVQZ	18.725	16.699	18.491	18.438	18.553	
aug-cc-pCV5Z	18.740	16.750	18.529	18.472		
C_{bb}						
cc-pCVDZ	58.729	49.887	53.101	52.922	53.055	52.945
cc-pCVTZ	63.368	53.207	57.122	56.305	56.540	
					(55.980)	(55.811)
cc-pCVQZ	63.980	53.545	57.487	56.497	56.736	
cc-pCV5Z	63.901	53.436	57.420	56.376		
aug-cc-pCVTZ	63.187	52.269	56.396	55.400	55.637	
aug-cc-pCVQZ	63.877	53.128	57.204	56.150	56.391	
aug-cc-pCV5Z	63.925	53.241	57.324	56.248		
C_{cc}						
cc-pCVDZ	23.638	21.493	22.344	22.375	22.433	22.409
cc-pCVTZ	25.270	23.059	24.121	23.958	24.037	
					(23.806)	(23.772)
cc-pCVQZ	25.646	23.406	24.465	24.259	24.342	
cc-pCV5Z	25.674	23.446	24.503	24.286		
aug-cc-pCVTZ	25.385	23.018	24.112	23.916	23.999	
aug-cc-pCVQZ	25.692	23.375	24.451	24.233	24.318	
aug-cc-pCV5Z	25.707	23.419	24.497	24.272		

[a]Values in parentheses obtained from calculations using the frozen-core approximation.

TABLE III. Computed ^{33}S spin–rotation constants (in kHz) for SO_2.[a]

	RHF	MP2	CCSD	CCSD(T)	CCSDT	CCSDTQ
C_{aa}						
cc-pCVDZ					(39.384)	(39.004)
cc-pCVTZ	49.899	35.902	40.660	38.737	38.957	
cc-pCVQZ	49.511	36.089	40.798	38.898		
cc-pCV5Z	49.466	36.146	40.887	38.984		
aug-cc-pCVTZ	49.699	35.723	41.700	38.679		
aug-cc-pCVQZ	49.419	35.971	40.747	38.858		
aug-cc-pCV5Z	49.431	36.094	40.866	38.970		
C_{bb}						
cc-pCVDZ					(5.533)	(5.511)
cc-pCVTZ	6.462	5.621	5.874	5.736	5.740	
cc-pCVQZ	6.469	5.664	5.914	5.779		
cc-pCV5Z	6.475	5.674	5.926	5.791		
aug-cc-pCVTZ	6.465	5.609	5.871	5.732		
aug-cc-pCVQZ	6.474	5.657	5.912	5.777		
aug-cc-pCV5Z	6.477	5.669	5.924	5.790		
C_{cc}						
cc-pCVDZ					(3.781)	(3.784)
cc-pCVTZ	4.203	4.345	4.244	4.251	4.246	
cc-pCVQZ	4.267	4.429	4.327	4.334		
cc-pCV5Z	4.267	4.439	4.336	4.343		
aug-cc-pCVTZ	4.202	4.337	4.236	4.241		
aug-cc-pCVQZ	4.264	4.424	4.322	4.328		
aug-cc-pCV5Z	4.267	4.437	4.335	4.342		

[a]Values in parentheses obtained from calculations using the frozen-core approximation.

TABLE IV. Vibrational corrections to the ^{33}S spin–rotation tensor (in kHz) and isotropic magnetic shielding (in ppm) of H_2S and SO_2 and to the ^{33}S shielding constant (in ppm) of OCS.

	C_{aa}	C_{bb}	C_{cc}	σ
$H_2{}^{33}S$				
fc-CCSD(T)/cc-pVTZ	2.751	2.391	−0.142	−19.7
fc-CCSD(T)/cc-pVQZ	2.696	2.250	−0.140	−19.0
CCSD(T)/cc-pCVTZ	2.947	2.517	−0.168	−20.5
CCSD(T)/cc-pCVQZ	2.884	2.396	−0.179	−19.9
CCSD(T)/aug-cc-pCVTZ	2.868	2.390	−0.167	−20.0
CCSD(T)/aug-cc-pCVQZ	2.854	2.373	−0.184	−19.7
$^{33}SO_2$				
fc-CCSD(T)/cc-pVTZ	0.282	0.009	−0.002	−8.3
fc-CCSD(T)/cc-pVQZ	0.289	0.010	−0.002	−8.2
CCSD(T)/cc-pCVTZ	0.308	0.007	−0.003	−8.3
$OC^{33}S$				
fc-CCSD(T)/cc-pVTZ				−13.6
fc-CCSD(T)/cc-pVQZ				−13.4
CCSD(T)/cc-pCVTZ				−14.3
CCSD(T)/cc-pCVQZ				−14.0

aug-cc-pCV*X*Z hierarchy shows a faster convergence to the CBS limit than does the cc-pCV*X*Z series. From fc-CCSD(T)/(aug)-cc-pCV5Z calculations (not reported in the tables), the magnitude of core-correlation effects is estimated at 1% to 3%. Finally, from Table II, it is evident that the double-zeta (DZ) basis sets are unsuitable for accurate calculations, showing deviations up to a few kHz. Nevertheless, such calculations are useful for estimating the contributions of higher than triple excitations.

To improve the accuracy of the computed spin–rotation constants further, a best estimate is derived as explained in the section "Quantum-chemical calculations". We note that the corrections due to a full treatment of triple excitations (i.e., the differences between CCSDT and CCSD(T)) are of the order of 0.5%, whereas the contributions due quadruple excitations are two to five times smaller.

For a comparison of our best-estimate *ab initio* values with experiment, it is mandatory to correct for molecular vibrations. Table IV contains the computed zero-point vibrational contributions to spin–rotation constants and isotropic shieldings for H_2S and SO_2. As noted in Ref. 57, for example, the magnitude of the vibrational corrections varies considerably among the individual components of the spin–rotation tensors. For H_2S, they amount to 15% for C_{aa}, 4% for C_{bb}, and less than 1% for C_{cc}. The vibrational contributions are smaller for SO_2 with corresponding corrections within 1% for all components and decreasing from 0.7% for C_{aa} to 0.05% for C_{cc}. As expected from the presence of hydrogen atoms in H_2S, the vibrational corrections are an order of magnitude larger for H_2S than for SO_2.

For both molecules, the vibrational contributions increase the values of C_{aa} and C_{bb}, while C_{cc} is decreased. The vibrationally corrected best estimates for the spin–rotation constants are listed in Table I; their good agreement with experiment has already been noted.

TABLE V. Calculated isotropic ^{33}S shielding constants (in ppm) for H_2S.

	RHF	MP2	CCSD	CCSD(T)	CCSDT	CCSDTQ
cc-pCVDZ	735.9	774.2	758.1	758.0	757.1	757.1
cc-pCVTZ	715.0	756.8	737.4	740.4	739.1	
cc-pCVQZ	711.9	755.0	735.6	739.3	738.0	
cc-pCV5Z	712.3	755.7	736.1	740.0		
aug-cc-pCVTZ	716.4	761.8	741.4	745.0	743.7	
aug-cc-pCVQZ	712.7	757.5	737.3	741.3	740.0	
aug-cc-pCV5Z	712.5	757.0	736.8	740.8		

^{33}S shielding constants

Tables V–VII contain the results of the electron-correlation and basis-set investigations of the isotropic magnetic ^{33}S shielding constants of H_2S, SO_2, and OCS, respectively. On the whole, the trends observed here follow the same patterns as for the spin–rotation constants—a smooth convergence is noted with respect to both electron-correlation treatment and basis-set effects. As for the spin–rotation constants, the best estimates are obtained by correcting the CCSD(T)/aug-cc-pCV5Z results for the neglected full triple and quadruple excitations. The resulting best estimates are 739.5 ppm for H_2S, −163.9 ppm for SO_2, and 803.3 ppm for OCS. Together with the computed zero-point vibrational correction of −19.7 ppm (CCSD(T)/aug-cc-pCVQZ value, see Table IV), the sulfur shielding of H_2S amounts to 719.8 ppm at 0 K; the additional inclusion of a temperature correction leads to a shielding of 719.0 ppm at 300 K. For SO_2, zero-point vibrational and temperature corrections lead to shieldings of −172.2 and −173.2 ppm at 0 and 300 K, respectively. The corresponding shielding values for OCS are 803.3 ppm at the geometrical equilibrium, 789.3 ppm at 0 K, and 787.9 ppm at 300 K, respectively.

^{33}S NMR shielding scale

The availability of accurate experimental values of the ^{33}S spin–rotation constants of H_2S enables the determination of a new, improved sulfur shielding scale. The procedure followed is well established and described several times in the literature.[1,2,57,58] Table VIII summarizes the various contributions needed for this analysis.

The starting point is the experimental isotropic spin–rotation constant, −35.41(49) kHz, as obtained from the individual components for the spin–rotation tensor reported in Table I for H_2S. The assumed error of 0.49 kHz is a conservative estimate, based on the squared sum of the errors in the individual components. The equilibrium value of −33.46(49) kHz is next obtained by subtracting the vibrational contribution, the latter being determined in CCSD(T)/aug-cc-pCVQZ calculations (see Table IV). Using Eq. (4), the equilibrium spin-rotation constant is converted to a value of −328.6(4.6) ppm for the paramagnetic part of the isotropic shielding constant. When the latter is combined with the computed diamagnetic contribution of 1065.5 ppm from CCSD(T)/aug-cc-pCV5Z calculations, we obtain 736.9(4.6) ppm for the equilibrium isotropic ^{33}S shielding constant.

Adding a vibrational correction of −19.7 ppm (CCSD(T)/aug-cc-pCVQZ calculations, see Table IV), we obtain the vibrationally averaged value of 717.2(4.6) ppm at 0 K. The temperature correction of −0.8 ppm at 300 K is an order of magnitude smaller but not entirely negligible. We thus arrive at a final value for the sulfur shielding constant of 716.4(4.6) ppm at 300 K, which is also our proposed reference point for a revised sulfur shielding scale. The error of ±5 ppm is due to the uncertainty associated with the experimental values for the diagonal components of the spin–rotation tensor.

We note that the derived "experimental" value of 716.4(4.6) ppm for the sulfur shielding constant of H_2S is in good agreement with our purely theoretical shielding value of 719.0 ppm, demonstrating the consistency of our results and the usefulness of our proposed scale. Nevertheless, we

TABLE VI. Calculated isotropic ^{33}S shielding constants (in ppm) for SO_2.[a]

	RHF	MP2	CCSD	CCSD(T)	CCSDT	CCSDTQ
cc-pCVDZ					(−109.6)	(−103.8)
cc-pCVTZ	−334.1	−119.1	−185.6	−153.5	−156.0	
cc-pCVQZ	−335.1	−131.1	−196.7	−165.1		
cc-pCV5Z	−335.0	−133.1	−199.2	−167.6		
aug-cc-pCVTZ	−331.9	−115.8	−183.9	−152.0		
aug-cc-pCVQZ	−334.2	−128.8	−195.6	−164.0		
aug-cc-pCV5Z	−334.7	−132.1	−198.8	−167.2		

[a]Values in parentheses obtained from calculations using the frozen-core approximation.

TABLE VII. Calculated isotropic ^{33}S shielding constants (in ppm) for OCS.[a]

	RHF	MP2	CCSD	CCSD(T)	CCSDT	CCSDTQ
cc-pCVDZ					(823.5)	(823.5)
cc-pCVTZ	795.3	824.5	805.5	806.8	805.5	
cc-pCVQZ	796.0	822.5	804.1	805.1		
cc-pCV5Z	795.5	821.5	803.4	804.3		
aug-cc-pCVTZ	797.0	826.6	807.6	808.7	807.4	
aug-cc-pCVQZ	795.8	822.7	804.2	805.2		
aug-cc-pCV5Z	795.7	822.0	805.2	804.6		

[a]Values in parentheses obtained from calculations using the frozen-core approximation.

TABLE VIII. Experimental ^{33}S shielding of $H_2{}^{33}S$ together with the corresponding spin–rotation constants, diamagnetic and paramagnetic parts of the shielding, as well as vibrational and temperature corrections.

Parameter			
$C^0_{\rm iso}$	(kHz)	−35.14(49)	Expt., see Table I
$C^e_{\rm iso}$	(kHz)	−33.46(49)	CCSD(T)/aug-cc-pCVQZ
$\sigma^{p,e}_{\rm iso}$	(ppm)	−328.6(4.6)	Expt., see Eq. (4)
$\sigma^{d,e}_{\rm iso}$	(ppm)	1065.5	CCSD(T)/aug-cc-pCV5Z
$\sigma^{e}_{\rm iso}$	(ppm)	736.9(4.6)	
$\Delta\sigma^{\rm vib}_{\rm iso}$	(ppm)	−19.7	CCSD(T)/aug-cc-pCVQZ
$\sigma^0_{\rm iso}$(T = 0 K)	(ppm)	717.2	
$\Delta\sigma^{T}_{\rm iso}$	(ppm)	−0.8	CCSD(T)/aug-cc-pCVQZ
$\sigma^0_{\rm iso}$(T = 300 K)	(ppm)	716.4(4.6)	

emphasize that the present procedure leads to a non-relativistic shielding constant of H_2S and a non-relativistic ^{33}S shielding scale. This can be considered unsatisfactory, bearing in mind that, for H_2S, for instance, the relativistic correction to the sulfur shielding is about 25 ppm and thus not negligible.[59] However, the present procedure yields a consistent non-relativistic description based on Eq. (4), establishing a useful link between non-relativistic NMR shielding calculations and experiment. A revision of the sulfur shielding scale based on a recently formulated relativistic relationship between the spin–rotation and nuclear magnetic shielding tensors[60] may be envisioned for the future, but the resulting shielding scale then provides the appropriate link between experiment and relativistic nuclear magnetic shielding calculations.

Returning to the sulfur scale proposed by Jackowski *et al.*,[5] we note that a direct comparison of the two scales is not straightforward due to the use of different reference compounds. A conversion is in principle possible using available experimental values for the relative shifts,[5] but unfortunately only a few gas-phase ^{33}S data are available in the literature[61] and liquid-phase values are less useful, being strongly affected by intermolecular interactions. For this reason, we carried out additional chemical-shift calculations for OCS, the reference compound chosen by Jackowski *et al.*,[5] see Table VII.

As it turns out, our computed ^{33}S shielding of OCS is significantly lower (by about 28 ppm) than the value (817(12) ppm) given by Jackowski *et al.*[5] as well as the theoretical value (809.05 ppm) given in Ref. 4, based on extensive multiconfigurational self-consistent-field calculations. Our computations furthermore provide a relative shift of 65 ppm between H_2S and OCS. The shielding scale proposed in the present work thus leads to a value of 781.2(6) ppm for the sulfur shielding of OCS, again substantially lower than the values reported in Refs. 4 and 5.

SUMMARY

Using the Lamb-dip technique, the hyperfine structure in the rotational spectra of $H_2{}^{33}S$ and $^{33}SO_2$ has been resolved. Their analysis, guided by high-level quantum-chemical coupled-cluster calculations, led to the determination of the corresponding hyperfine parameters. The good agreement between theory and experiment for these parameters confirms the reliability of the determined values. With respect to the available data in the literature, the present work allowed us to improve the accuracy for the sulfur spin–rotation constants of $^{33}SO_2$ and to revise completely the spin–rotation constants for $H_2{}^{33}S$; those reported in the literature turned out to be incorrect.

The ^{33}S spin–rotation tensor of H_2S was subsequently used to establish a new experimental sulfur shielding scale. The shielding derived in this way for H_2S, 716(5) ppm, is in good agreement with the corresponding theoretical results, provided that they have been obtained with an adequate treatment of electron correlation in a sufficiently large basis set. The zero-order vibrational correction of about −20 ppm is substantial, while the temperature correction of about −1 ppm is small but not negligible. The agreement obtained between theory and experiment suggests that the present scale can be considered reliable and of good accuracy.

However, a discrepancy is noted relative to a sulfur shielding scale of Jackowski *et al.*,[4,5] based on the ^{33}S spin–rotation constant of OCS. The superiority of the present result is supported by quantum-chemical calculations for the shielding constant of OCS, which, consistent with the new scale, suggest that the previous scale is too high by about 30 ppm. We thus recommend that the sulfur shielding scale be based in the future on our shielding value of 716(5) ppm for H_2S rather than on the shielding constant of OCS.

Clearly, the fact that only a few gas-phase ^{33}S NMR measurements have been reported so far[61] restricts the applicability of the present sulfur scale somewhat—in particular, as no NMR data for gaseous H_2S have been reported. Such a measurement may nevertheless be useful to connect the sulfur shielding determined in this work for H_2S with the available ^{33}S NMR data. Gas-phase measurements are also warranted in order to investigate the role of intermolecular interactions in some detail, as there exists some evidence that sulfur shifts are rather sensitive to environmental effects.[61] Finally, we note that our shielding scale has been derived within a non-relativistic framework based on Eq. (4). In this way, it provides a useful link between experiment and the non-relativistic shielding calculations that are usually performed in chemical applications. The inclusion of relativistic effects, following recent work on the relativistic calculation of spin–rotation constants, may give further insight into the relationship between spin–rotation and shielding tensors. However, the relativistic corrections are expected to be small for the sulfur spin–rotation constants.

ACKNOWLEDGMENTS

This work has been supported in Oslo by the CoE Centre for Theoretical and Computational Chemistry through Grant No. 179568/V30 and in Mainz by the Deutsche Forschungsgemeinschaft (DFG GA 370/5-1) and the Fonds der Chemischen Industrie as well as in Bologna by MIUR (PRIN 2009 funds) and by the University of Bologna (RFO funds).

[1] C. J. Jameson, Chem. Rev. **91**, 1375 (1991).
[2] D. L. Bryce and R. E. Wasylishen, Acc. Chem. Res. **36**, 327 (2003).
[3] A. M. Teale, O. B. Lutnæs, T. Helgaker, D. J. Tozer, and J. Gauss, J. Chem. Phys. **138**, 024111 (2013).
[4] J. Jackowski, M. Jaszuński, W. Makulski, and J. Vaara, J. Magn. Reson. **135**, 444 (1998).
[5] J. Jackowski, W. Makulski, and W. Koźmiński, Magn. Reson. Chem. **40**, 563 (2002).
[6] J. M. L. J. Reinartz and A. Dymanus, Chem. Phys. Lett. **24**, 346 (1974).
[7] R. E. Wasylishen, C. Connor, and J. O. Friedrich, Can. J. Chem. **62**, 981 (1984).
[8] G. Cazzoli and C. Puzzarini, J. Mol. Spectrosc. **240**, 153 (2006).
[9] C. Puzzarini, G. Cazzoli, and J. Gauss, J. Chem. Phys. **137**, 154311 (2012).
[10] C. C. Costain, Can. J. Phys. **47**, 2431 (1969).
[11] R. S. Winton and W. Gordy, Phys. Lett. A **32**, 219 (1970).
[12] G. Cazzoli and L. Dore, J. Mol. Spectrosc. **143**, 231 (1990).
[13] L. Dore, C. Degli Esposti, A. Mazzavillani, and G. Cazzoli, Chem. Phys. Lett. **300**, 489 (1999).
[14] G. Cazzoli and L. Dore, J. Mol. Spectrosc. **141**, 49 (1990).
[15] L. Dore, J. Mol. Spectrosc. **221**, 93 (2003).
[16] G. Cazzoli, C. Puzzarini, and A. V. Lapinov, Astrophys. J. **611**, 615 (2004).

[17]D. A. Landman, R. Roussel-Dupré, and G. Tanigawa, Astrophys. J. **261**, 732 (1982).
[18]H. S. P. Müller, J. Farhoomand, E. A. Cohen, B. Brupbacher-Gatehouse, M. Schäfer, A. Bauder, and G. Winnewisser, J. Mol. Spectrosc. **201**, 1 (2000).
[19]G. Cazzoli and C. Puzzarini, "The rotational spectrum of hydrogen sulfide: The $H_2{}^{32}S$ and $H_2{}^{33}S$ isotopologues," J. Mol. Spectrosc. (submitted).
[20]H. M. Pickett, J. Mol. Spectrosc. **148**, 371 (1991).
[21]H. M. Pickett, SPFIT/SPCAT package, see http://spec.jpl.nasa.gov.
[22]J. K. G. Watson, in *Vibrational Spectra and Structure*, edited by J. R. Durig (Elsevier, New York/Amsterdam, 1977), Vol. 6.
[23]T. Helgaker, K. Ruud, and M. Jaszuński, Chem. Rev. **99**, 293 (1999).
[24]J. Gauss and J. F. Stanton, Adv. Chem. Phys. **123**, 355 (2002).
[25]W. H. Flygare, J. Chem. Phys. **42**, 1157 (1965).
[26]W. H. Flygare, Chem. Rev. **74**, 653 (1974).
[27]F. London, J. Phys. Radium **8**, 397 (1937).
[28]K. Wolinski, J. F. Hinton, and P. Pulay, J. Am. Chem. Soc. **112**, 8251 (1990).
[29]J. Gauss, K. Ruud, and T. Helgaker, J. Chem. Phys. **105**, 2804 (1996).
[30]G. D. Purvis III and R. J. Bartlett, J. Chem. Phys. **76**, 1910 (1982).
[31]J. Noga and R. J. Bartlett, J. Chem. Phys. **86**, 7041 (1987).
[32]G. E. Scuseria and H. F. Schaefer III, Chem. Phys. Lett. **152**, 382 (1988).
[33]M. Kállay and P. R. Surján, J. Chem. Phys. **115**, 2945 (2001).
[34]C. Møller and M. S. Plesset, Phys. Rev. **46**, 618 (1934).
[35]K. Raghavachari, G. W. Trucks, J. A. Pople, and M. Head-Gordon, Chem. Phys. Lett. **157**, 479 (1989).
[36]J. F. Stanton, J. Gauss, M. E. Harding, P. G. Szalay with contributions from A. A. Auer, R. J. Bartlett, U. Benedikt, C. Berger, D. E. Bernholdt, Y. J. Bomble, L. Cheng, O. Christiansen, M. Heckert, O. Heun, C. Huber, T.-C. Jagau, D. Jonsson, J. Jusélius, K. Klein, W. J. Lauderdale, D. A. Matthews, T. Metzroth, L. A. Mück, D. P. O'Neill, D. R. Price, E. Prochnow, C. Puzzarini, K. Ruud, F. Schiffmann, W. Schwalbach, S. Stopkowicz, A. Tajti, J. Vázquez, F. Wang, J. D. Watts, and the integral packages MOLECULE (J. Almlöf and P. R. Taylor), PROPS (P. R. Taylor), ABACUS (T. Helgaker, H. J. Aa. Jensen, P. Jørgensen, and J. Olsen), and ECP routines by A. V. Mitin and C. van Wüllen. For the current version, see http://www.cfour.de.
[37]See www.mrc.hu, a quantum-chemical program suite written by M. Kállay.
[38]M. Heckert, M. Kállay, D. P. Tew, W. Klopper, and J. Gauss, J. Chem. Phys. **125**, 044108 (2006).
[39]D. Feller, J. Chem. Phys. **98**, 7059 (1993).
[40]T. H. Dunning, Jr., J. Chem. Phys. **90**, 1007 (1989).
[41]A. K. Wilson, T. van Mourik, and T. H. Dunning, Jr., J. Mol. Struct.: THEOCHEM **388**, 339 (1996).
[42]D. E. Woon and T. H. Dunning, Jr., J. Chem. Phys. **98**, 1358 (1993).
[43]T. van Mourik and T. H. Dunning, Jr., Int. J. Quantum Chem. **76**, 205 (2000).
[44]T. Helgaker, W. Klopper, H. Koch, and J. Noga, J. Chem. Phys. **106**, 9639 (1997).
[45]I. M. Mills, in *Molecular Spectroscopy: Modern Research*, edited by K. N. Rao and C. W. Matthews (Academic, New York, 1972), p. 115.
[46]A. A. Auer, J. Gauss, and J. F. Stanton, J. Chem. Phys. **118**, 10407 (2003).
[47]S. Stopkowicz and J. Gauss, "Revised values for the nuclear quadrupole moments of ^{33}S and ^{35}S," Phys. Rev. A (to be published).
[48]J. Gauss, Chem. Phys. Lett. **191**, 614 (1992).
[49]J. Gauss and J. F. Stanton, J. Chem. Phys. **102**, 251 (1995).
[50]J. Gauss and J. F. Stanton, J. Chem. Phys. **104**, 2574 (1996).
[51]J. Gauss, J. Chem. Phys. **116**, 4773 (2002).
[52]M. Kállay and J. Gauss, J. Chem. Phys. **120**, 6841 (2004).
[53]D. E. Woon and T. H. Dunning, Jr., J. Chem. Phys. **103**, 4572 (1995).
[54]K. A. Peterson and T. H. Dunning, Jr., J. Chem. Phys. **117**, 10548 (2002).
[55]R. A. Kendall, T. H. Dunning, Jr., and R. J. Harrison, J. Chem. Phys. **96**, 6796 (1992).
[56]A. H. Saleck, M. Tanimoto, S. P. Belov, T. Klaus, and G. Winnewisser, J. Mol. Spectrosc. **171**, 481 (1995).
[57]C. Puzzarini, G. Cazzoli, M. E. Harding, J. Vázquez, and J. Gauss, J. Chem. Phys. **131**, 234304 (2009).
[58]D. Sundholm, J. Gauss, and A. Schäfer, J. Chem. Phys. **105**, 11051 (1996).
[59]P. Manninen, K. Ruud, P. Lantto, and J. Vaara, J. Chem. Phys. **122**, 114107 (2005).
[60]E. Malkin, S. Komorovsky, M. Repisky, T. B. Demissie, and K. Ruud, J. Phys. Chem. Lett. **4**, 459 (2013).
[61]W. Makulski and K. Jackowski, J. Mol. Struct. **704**, 219 (2004).